

THE OBLIQUITY OF JUPITER

WILLIAM R. WARD AND ROBIN M. CANUP

Southwest Research Institute, 1050 Walnut Street, Suite 400, Boulder, CO 80302
 Received 2005 August 11; accepted 2006 February 3; published 2006 February 28

ABSTRACT

The spin-axis precession period of Jupiter is near that of a fundamental Laplace-Lagrange solar system mode describing the precession of Uranus’s orbit plane ($\sim 4.3 \times 10^5$ yr). As a result, a portion of the $3^\circ 1'$ obliquity of Jupiter may actually be forced by a spin-orbit secular resonance with Uranus. If this portion predominates, it allows for a constraint on Jupiter’s moment of inertia that is independent of interior models.

Subject headings: celestial mechanics — planets and satellites: individual (Jupiter) — solar system: general

1. INTRODUCTION

It is a remarkable occurrence in the solar system that the spin-axis precession periods of Jupiter [$\approx 4.74(\lambda/0.25) \times 10^5$ yr] and Saturn [$\approx 1.75(\lambda/0.22) \times 10^6$ yr] are correspondingly very close to the precession periods of the orbit planes of Uranus (4.33×10^5 yr) and Neptune (1.87×10^6 yr), where λ is the normalized moment of inertia of the planet (Ward 1974; Harris & Ward 1982). Such near-commensurability can result in strong spin-orbit interactions, and indeed, Neptune perturbations may be responsible for the large $26^\circ 7'$ obliquity of Saturn. Ward & Hamilton (2004, hereafter WH; see also Hamilton & Ward 2004, hereafter HW) suggest that Saturn and Neptune currently occupy a secular spin-orbit resonance and propose that Saturn initially formed with a small obliquity but later acquired its current value by means of resonance capture as the Kuiper Belt was depleted, Neptune migrated, or both.

In this Letter, we concentrate on Jupiter, whose spin-axis precession rate is suspiciously close to the precession rate of the principal Laplace-Lagrange mode controlling Uranus’s orbit plane (Ward 1974; Harris & Ward 1982). Following the procedure outlined in WH for locating the spin axis in a reference plane rotating with the mode’s frequency, one also finds that the longitude of Jupiter’s north pole is nearly aligned with the effective orbit normal of this mode (D. P. Hamilton 2004, private communication). This may indicate that a significant portion of Jupiter’s spin-axis motion is being forced by Uranian perturbations. If so, this would have important implications for Jupiter’s moment of inertia, C . Typically, a value of C is derived from Jupiter’s J_2 and is then dependent on the adopted planetary-interior model. Thus, an independent value for C would render the measured J_2 more diagnostic of other aspects of interior structure, including a possible Jovian core, whose presence has key implications for Jupiter’s origin (W. B. Hubbard 2005, private communication). Here we offer such an estimate based solely on the spin dynamics of the planet and its potentially strong interactions with Uranus.

2. PRECESSIONAL EQUATIONS

Spin axis.—The equation of motion for a planet’s unit spin-axis vector, s , is $ds/dt = \alpha(s \cdot n)(s \times n)$, where n is the unit vector normal to the planet’s orbit plane. The precession rate α depends on the strength of the solar torque exerted on the planet and its spin angular momentum. For Jupiter, most of the torque is actually exerted on the Galilean satellites instead of directly on the planet (Ward 1975), although Jupiter’s large quadrupole gravity field locks the satellites to its equatorial

plane so that the system precesses as a unit (Goldreich 1965). The precessional constant, α , can be written

$$\alpha = \frac{3}{2} \frac{GM_\odot}{\omega a_j^3} \left(\frac{J_2 + q}{\lambda + l} \right), \quad (1)$$

(Ward 1975; French et al. 1993; WH), where $\omega = 1.7587 \times 10^{-4} \text{ s}^{-1}$ is the spin frequency of Jupiter, $a_j = 5.2028 \text{ AU}$ is its heliocentric distance, J_2 is the quadrupole coefficient of its gravity field, and $\lambda \equiv C/M_j R^2$. The quantity $q \equiv \frac{1}{2} \sum_j (m_j/M_j)(a_j/R)^2$ is an effective quadrupole coefficient of the satellite system, and $l \equiv \sum_j m_j (GM_j a_j)^{1/2} / M_j R^2 \omega$ is the angular momentum of the satellite system normalized to $M_j R^2 \omega$, where M_j and R are the mass and radius of Jupiter and $\{m_j, a_j\}$ are the masses and orbital radii of its satellites. Jupiter system data compiled by D. R. Williams¹ list $\lambda = 0.254$ and $J_2 = 0.01469$, as well as satellite masses and orbital distances that we use to find $q = 0.03033$ and $l = 0.00263$. With these numbers, equation (1) yields $\alpha = 2''.741 \text{ yr}^{-1}$.

Orbit plane.—If the orbit plane of Jupiter were fixed in inertial space, the spin axis would precess uniformly with a period $P = 2\pi/(\alpha \cos \epsilon) = 4.735 \times 10^5 \text{ yr}$, where $\epsilon = 3^\circ 12'$ is the Jovian obliquity. However, the orbit plane of Jupiter is not fixed; all of the planetary orbits have small inclinations to the invariable plane of the solar system and undergo nonuniform regression of their orbital nodes due to their mutual gravitational perturbations. The orbital inclination I and ascending node Ω of a given planet are then found from a superposition

$$\begin{aligned} \sin \frac{I}{2} \sin \Omega &= \sum_j \frac{I_j}{2} \sin (g_j t + \delta_j), \\ \sin \frac{I}{2} \cos \Omega &= \sum_j \frac{I_j}{2} \cos (g_j t + \delta_j) \end{aligned} \quad (2)$$

(e.g., Brouwer & van Woerkom 1950; Bretagnon 1974; Aplegate et al. 1986, hereafter A86), comprising many terms of amplitudes $\{I_j\}$ and frequencies $\{g_j\}$. A86 provide the amplitudes, frequencies, and phase constants of 20 such terms for Jupiter as found from their numerical integrations. The largest amplitude terms (i.e., $j = 3, 6,$ and 14 when ordered by increasing frequency) represent contributions from three of the eight fundamental inclination modes of the Laplace-Lagrange secular evolution of the solar system. The first of these ($I_3 = 0''.0659$, $g_3 = -0''.692 \text{ yr}^{-1}$, $\delta_3 = 235^\circ 203'$) is due to the

¹ See <http://nssdc.gsfc.nasa.gov/planetary/factsheet/jupiterfact.html>.

$2\pi/|g_3| = 1.87 \times 10^6$ yr nodal regression of Neptune and the second ($I_6 = 0^{\circ}0548$, $g_6 = -2^{\circ}995 \text{ yr}^{-1}$, $\delta_6 = 140^{\circ}203$) to that of Uranus ($2\pi/|g_6| = 4.33 \times 10^5$ yr), while the last ($I_{14} = 0^{\circ}362$, $g_{14} = -26^{\circ}332 \text{ yr}^{-1}$, $\delta_{14} = 307^{\circ}357$) is due to the $2\pi/|g_{14}| = 4.92 \times 10^4$ yr mutual orbital precession of Jupiter and Saturn.

3. SPIN-AXIS MOTION

A nonuniform precession of the orbit leads to oscillations of the planet's obliquity as the spin axis attempts to respond to the moving orbit normal $\mathbf{n}(t)$. In component form, the spin-axis motion can be written $\dot{s}_x = \alpha(\mathbf{s} \cdot \mathbf{n})(s_y n_z - s_z n_y)$, $\dot{s}_y = -\alpha(\mathbf{s} \cdot \mathbf{n})(s_x n_z - s_z n_x)$, and $\dot{s}_z = \alpha(\mathbf{s} \cdot \mathbf{n})(s_x n_y - s_y n_x)$, where $\{s_i, n_i\}$ denote the components of the unit vectors with respect to the invariable plane of the solar system. To first-order accuracy in small angles, we can set $\mathbf{s} \cdot \mathbf{n} \approx n_z \approx s_z \approx 1$, to reduce the first two equations to $\dot{s}_x = \alpha(s_y - n_y)$ and $\dot{s}_y = -\alpha(s_x - n_x)$ while dropping the third. Differentiating the second equation and using the first to eliminate \dot{s}_x then leads to $d^2 s_y / dt^2 + \alpha^2 s_y = \alpha(\alpha n_y + \dot{n}_x)$, which is the equation for a forced harmonic oscillator. This has both a homogeneous solution, $s_{x,h} = \theta_h \cos(-\alpha t + \delta)$, $s_{y,h} = \theta_h \sin(-\alpha t + \delta)$ with constants θ_h and δ to be determined from observations, and a particular solution

$$\begin{aligned} s_{x,p} &= \sum_j \frac{\alpha I_j}{\alpha + g_j} \cos\left(g_j t + \delta_j - \frac{\pi}{2}\right), \\ s_{y,p} &= \sum_j \frac{\alpha I_j}{\alpha + g_j} \sin\left(g_j t + \delta_j - \frac{\pi}{2}\right), \end{aligned} \quad (3)$$

where we have set $\sin(I_j/2) \approx I_j/2$ and identified $n_x = \sum_j I_j \cos(g_j t + \delta_j - \pi/2)$ and $n_y = \sum_j I_j \sin(g_j t + \delta_j - \pi/2)$, recalling that the orbit normal lags the ascending node by 90° . In the limit that $\alpha \gg \{|g_j|\}$, $s_{x,p} \rightarrow n_x$ and $s_{y,p} \rightarrow n_y$, which is the well-known result that a rapidly precessing planet "follows" its orbit normal.

The amplitude θ_h represents the free part of the spin-axis motion. In the absence of a free component, equation (3) gives the forced position of the spin axis due to the motion of the orbit plane. For small angles, the tilt of the spin axis to the invariable-plane normal is $\theta \approx (s_x^2 + s_y^2)^{1/2}$, whereas the obliquity is $\epsilon \approx [(s_x - n_x)^2 + (s_y - n_y)^2]^{1/2}$.

For Jupiter, the closeness of its spin-axis precession rate α to the Uranus orbit precession rate $-g_6$ and the relatively large value of I_6 make the amplitude of the $j = 6$ term's contribution to the spin-axis motion greatly enhanced. This suggests we view the motion of both the Jovian spin axis and orbit normal from a frame rotating with that frequency (WH).² The particular solution in this frame now reads

$$\begin{aligned} s'_{x,p} &= -\frac{\alpha I_6}{\alpha + g_6} + \sum_{j \neq 6} \frac{\alpha I_j}{\alpha + g_j} \cos[(g_j - g_6)t + \phi_j], \\ s'_{y,p} &= \sum_{j \neq 6} \frac{\alpha I_j}{\alpha + g_j} \sin[(g_j - g_6)t + \phi_j], \end{aligned} \quad (4)$$

where the new phase $\phi_j = \delta_j - \delta_6 - \pi$. The time-varying part of equation (4) is dominated by the $j = 14$ term and is not

² To do this, we subtract a phase ($g_6 t + \delta_6 \sim \pi/2$) + π from the argument of each term, with the $+\pi$ term placing the $j = 6$ contribution on the new positive x -axis.

altered much for small changes in α . In contrast, because of its small denominator, the leading time-constant term is very sensitive to α and diverges as $\alpha + g_6 \rightarrow 0$.

Divergence occurs because the problem has been linearized. This singularity can be removed by replacing the lead term with a nonlinear guiding center obtained from Cassini state theory (e.g., Colombo 1966; Peale 1969, 1974; Ward et al. 1979). It turns out that the high-frequency terms do not interfere much with the motion of this guiding center (e.g., Ward 1992; HW), which is quite similar to a spin-axis motion in the case of uniform orbital precession (i.e., a single orbital term) with $I = I_6$ and $\Omega = g_6$. In this case, Cassini states are positions for which the guiding center can coprecess with the $j = 6$ term and appear stationary in the rotating frame. They all lie on the x -axis of the rotating frame at angular distances θ_c given by solutions of $\alpha \cos(\theta_c + I_6) \sin(\theta_c + I_6) + g_6 \sin \theta_c = 0$, which has either two or four solutions, depending on the ratio α/g_6 . One of these (Cassini state 3) is near 180° (retrograde) and will not concern us here, while state 4 lies on a separatrix and is unstable.³ States 1 and 2 are both stable. State 2 always exists and lies on the positive x -axis, while state 1 does not exist for $|\alpha/g_6| < (\sin^{2/3} I_6 + \cos^{2/3} I_6)^{3/2} = 1.0146$ (WH), which corresponds to $\alpha < 3.039$ and $\lambda > 0.2289$: the regime of interest here. Since state 1 positions would also be nearly antialigned in azimuth with the observed spin axis (on the negative x -axis), they will not be considered further. Assuming the forced pole is near state 2, we pick an angle θ_c , solve for the associated α (and therefore λ through eq. [1]), and then use it to evaluate the remainder of equation (4) to deduce the forced-pole behavior as a function of λ .⁴ Figure 1a displays the Jovian orbit normal and generalized Cassini state positions for the next 10^6 yr for two values, $\lambda = 0.254$ and $\lambda = 0.2365$. Figure 1b shows the current ($t = 0$) loci of the forced pole as the assumed λ of Jupiter is varied. These all lie at a near-constant distance, $s'_{y,p} \approx 0^{\circ}07$, below the x -axis due to the nonresonant terms.

4. POLE POSITION

Next we locate the actual Jovian north pole in our rotating frame. The right ascension and declination of s with respect to Earth's equator and equinox at epoch J2000.0 are $268^{\circ}05$ and $64^{\circ}49$, respectively (Cox 2000), and are given as the first entry in Table 1 as polar coordinates after replacing declination with colatitude. Rotating about the vernal equinox by Earth's obliquity, $23^{\circ}439$ (Yoder 1995), gives s with respect to the ecliptic and equinox. The normal \mathbf{k} to the invariable plane at J2000.0 is also given in this system by Cox (2000). Because the angles are so small, we can translate to the invariable plane by simply subtracting the x - y components of \mathbf{k} from s . The effective pole position \mathbf{n}_6 of the $j = 6$ term is also listed (which is 180° from the Uranus orbit normal; A86). A counterclockwise rotation of the coordinate system by $\pi - 50^{\circ}203$ then puts \mathbf{n}_6 on the new negative x -axis. In this system, the spin axis is tilted by $\theta = 3^{\circ}454$ and only $\phi_s = -2^{\circ}974$ below the positive x -axis. Its location is indicated in Figure 1b. The orbit normal is dominated by the $j = 14$ term due to Saturn and is included in the

³ The numbering and sign convention follow that of Peale (1974), except that we measure θ_c with respect to the normal of the invariable plane instead of the effective normal of the $j = 6$ term.

⁴ This can be considered a generalization of the Cassini state to nonuniform orbit precession (e.g., Ward & de Campli 1979), and a similar procedure has been used recently by Bills (2005) to examine the obliquities of the Galilean satellites and by Peale (2005) in the case of Mercury.

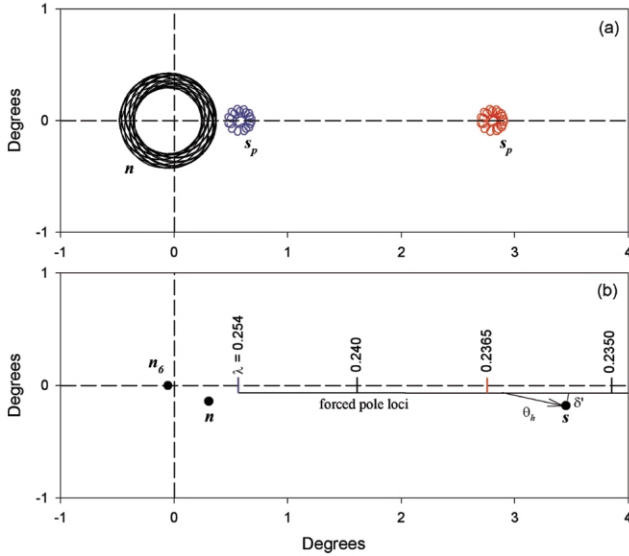


FIG. 1.—(a) Trajectories of the orbit normal (*black*) and the forced pole s_p (particular solution) for the next million years shown in a coordinate system rotating with a frequency $g_s = -2'995 \text{ yr}^{-1}$. Forced poles are shown for two moments of inertia: $\lambda = 0.254$ (*blue*) and $\lambda = 0.2365$ (*red*). The fine structure comes from the $j \neq 6$ terms, most notably the $j = 3$ (Neptune) and the $j = 14$ (Saturn). (b) The nearly straight-line loci (lying $y \approx -0'07$ below the positive x -axis) of the current forced pole for various values of λ . The present locations of Jupiter's spin axis s , orbit normal n , and effective normal of the Uranus perturbation of the Jovian orbit, n_6 , are shown. The amplitude θ_h and phase δ' of the free (homogeneous) solution are found by running a vector from any forced-pole position to the spin axis.

figure, so that the distance between s and the orbit normal n is the current $\epsilon = 3:12$ obliquity of Jupiter.

5. MOMENT OF INERTIA

Since the current spin-axis position could be a combination of forced and free motions, we cannot make a unique fit for θ_h , δ' , and α , where δ' is now the phase of the homogeneous solution in the rotating frame. Starting at any point along the line of possible generalized Cassini states $(s'_{x,p}, s'_{y,p})$, the amplitude and phase of the free contribution are given by the vector connecting that point with the observed pole (s'_x, s'_y) as shown in Figure 1b, so that

$$\theta_h = [(s'_x - s'_{x,p})^2 + (s'_y - s'_{y,p})^2]^{1/2},$$

$$\sin \delta' = (s'_y - s'_{y,p})/\theta_h. \tag{5}$$

Since the pole does not lie directly on the forced motion curve, Jupiter's free obliquity cannot be zero. Its minimum value $\theta_{\min} \approx |s'_y - s'_{y,p}| \approx 0:11$ occurs when $s'_x = 3:454 \cos(-2:974) \approx s'_{x,p}$, for which $\lambda \approx 0.2355$ and $\alpha \approx 2'96 \text{ yr}^{-1}$.

In Figure 2, we show the time evolution of the spin axis for the two values of λ used in Figure 1a, extending the integration to $t \sim 2\pi/|\alpha(\lambda = 0.2365) - g_6| \sim 24 \text{ Myr}$ to see the full range of motion. The further the forced solution is from the spin axis, the less likely it is that we should at any given time find the spin axis so near the generalized Cassini state line. The probability is of order $P \approx |\delta'|/180^\circ$ to find the spin axis $\pm |s'_y - s'_{y,p}|$ from that line and to the right of the forced pole. This rises to above 10% only for a free-obliquity amplitude $\theta_h < 0:35$. In Figure 3, we plot α , θ_c , θ_h , and P as functions of λ .

TABLE 1
COORDINATES OF JUPITER SPIN AXIS IN ROTATING FRAME

Reference Frame i	Vector	Colatitude (deg)	Longitude (deg)
Equator/equinox 1	s	25.51	268.05
Ecliptic/equinox 2	k	1.579	17.583
	s	2.223	247.78
Invariable plane 3	n_6	0.0548	50.203
	s	3.4544	227.23
Rotating system 4	n_6	0.0548	180.00
	s	3.4544	357.03

6. DISCUSSION

We have argued, on the basis of a near-alignment of Jupiter's north pole azimuth with that of Uranus's orbit normal on the invariable plane, that a significant portion of Jupiter's 3:12 obliquity may be caused by perturbations from Uranus. If so, Jupiter's normalized moment of inertia, $\lambda = C/M_J R^2$, would be several percent smaller than previous estimates, perhaps closer to 0.236. This is still within the theoretical envelope of possible values compatible with the measured value of J_2 (Hubbard 2005), although its additional compatibility with J_4 should also be examined (Guillot & Hueso 2005).⁵

On the other hand, coincidences do happen, and one cannot categorically rule out an accidental alignment. A measurement of the precession constant α would determine λ through equa-

⁵ Theoretical values of C range from ~ 0.255 for the extreme of a constant-density core and massless envelope to ~ 0.221 for a constant-density envelope and point-mass core (Hubbard 2005).

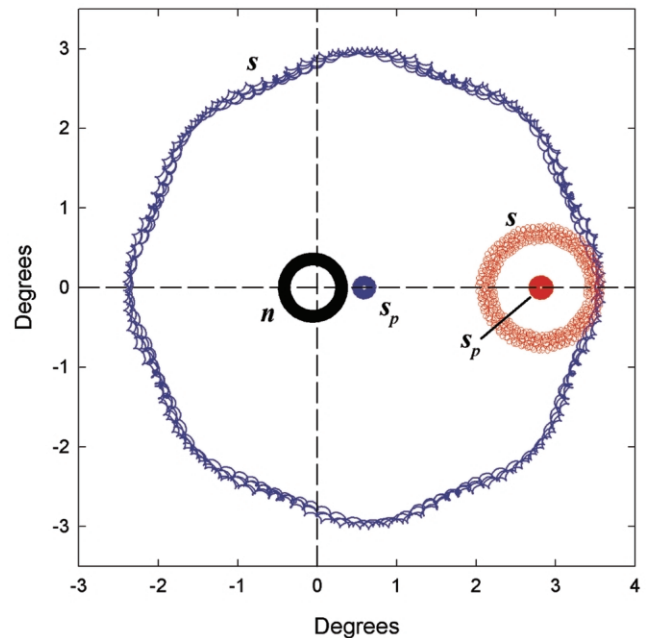


FIG. 2.—A 24 Myr trace of the spin-axis trajectory, s , for the two values of λ used in Fig. 1. If the forced pole is relatively far from the current s (e.g., *blue trajectory*), a large portion of the spin-axis motion must be due to a free component θ_h , and the spin axis spends most of its time well away from the x -axis. If the forced pole is near the current s (e.g., *red trajectory*), then θ_h is small and the spin axis never travels far from the x -axis in this rotating frame. Over the time interval of the plot, the homogeneous solution executes one cycle on the red curve but five cycles on the blue curve, where the prominent sculpting is due to Neptune perturbations. On a probability basis, the closeness of the spin axis to the forced-pole line (Fig. 1b) implies a predominantly forced Jovian obliquity.

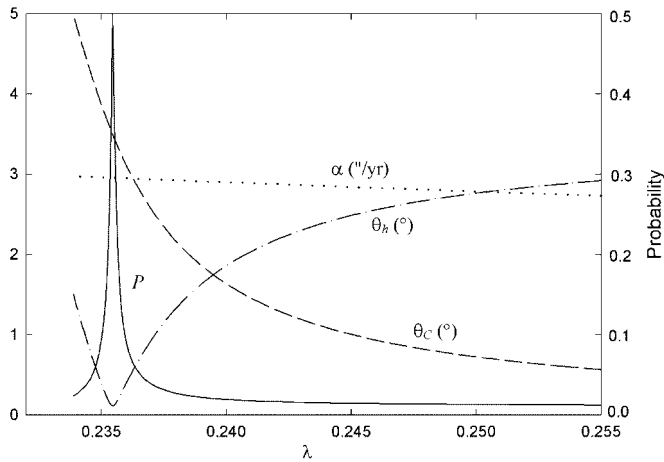


FIG. 3.—Spin-axis precession rate α , the $j = 6$ Cassini state distance θ_c , the free-component amplitude θ_n (left scale), and the probability P (right scale) as functions of the assumed moment of inertia constant for Jupiter, λ .

tion (1). In lieu of this, we have used the Cassini state angle as a proxy for α , but an ambiguity remains as to what portion of the Jovian obliquity is free versus forced. Direct measurement of the motion of the pole would allow a determination of λ through $\alpha = \dot{s}/(s \cdot \mathbf{n})(s \times \mathbf{n}) = 2|\Delta s|/(\Delta t \sin 2\epsilon)$, where Δs is the position change over time interval Δt . The *Juno* mission, planned for 2011, will add a number of data points for the Jupiter pole position over a time interval of ~ 1 yr, but the ultimate precision will depend on the length of the mission (W. Hubbard 2005, private communication). At least two-figure

accuracy would be needed to test whether the Jovian obliquity is primarily a forced response to Uranus.

Our estimates for λ depend on J_2 and ω , as well as on the frequency and phase constant of the $j = 6$ term and the Jovian pole position. Uncertainties in the rotational profile of the planet could also affect the estimate. Including the eccentricity of Jupiter's orbit only alters its spin-axis precession rate by a factor $(1 - e^2)^{-3/2} \approx 1.003$. The planetary model of Bretagnon (1974) lists a phase constant for the Uranus term of $136^\circ 29'$, resulting in a pole $\phi_s = 0^\circ 936'$ above the x -axis, but this does not significantly alter the probabilities. In the original treatment of solar system secular variations, Brouwer & van Woerkom (1950) obtained a value of $g_6 = -2''903 \text{ yr}^{-1}$, which for a given Cassini state distance θ_c would imply a larger λ by ~ 0.004 . However, the more recent value of Bretagnon (1974), $g_6 = -2''99984 \text{ yr}^{-1}$, is very close to the A86 result we have used.

Finally, a smaller free component than the present $3^\circ 12'$ obliquity implies that either Jupiter formed with a spin axis nearly perpendicular to its orbit plane or some as yet unknown damping mechanism has decayed the free obliquity. Damping could also affect the Cassini state position (Ward & de Campli 1979), but as it is likely that Saturn currently librates about its forced-pole position with an amplitude of $\sim 31^\circ$ (WH; HW), this seems to generally argue against such a damping mechanism.

The authors thank D. P. Hamilton for initially alerting us to the Jovian spin-axis position relative to the Cassini state associated with Uranus's perturbations, and W. Hubbard, D. Stevenson and J. Wisdom for helpful comments. This work was supported by NASA's Planetary Geology and Geophysics Program.

REFERENCES

- Applegate, J. H., Douglas, M. R., Gürsel, Y., Sussman, G. J., & Wisdom, J. 1986, *AJ*, 92, 176 (A86)
- Bills, B. G. 2005, *Icarus*, 175, 233
- Bretagnon, P. 1974, *A&A*, 30, 141
- Brouwer, D., & van Woerkom, A. J. J. 1950, *The Secular Variations of the Orbital Elements of the Principal Planets* (Astron. Pap. Am. Ephemeris Naut. Alm., 13, 81) (Washington: GPO)
- Colombo, G. 1966, *AJ*, 71, 891
- Cox, A. N., ed. 2000, *Allen's Astrophysical Quantities* (4th ed.; New York: AIP)
- French, R. G. et al. 1993, *Icarus*, 103, 163
- Goldreich, P. 1965, *AJ*, 70, 5
- Guillot, T., & Hueso, R. 2005, *BAAS*, 37, Div. Planet. Sci. abstr. No. 25.06
- Hamilton, D. P., & Ward, W. R. 2004, *AJ*, 128, 2510 (HW)
- Harris, A. W., & Ward, W. R. 1982, *Annu. Rev. Earth Planet. Sci.*, 10, 61
- Hubbard, W. B. 2005, *BAAS*, 37, Div. Planet. Sci. abstr. No. 34.01
- Peale, S. J. 1969, *AJ*, 74, 483
- . 1974, *AJ*, 79, 722
- . 2005, *Icarus*, 178, 4
- Ward, W. R. 1974, *J. Geophys. Res.*, 79, 3375
- . 1975, *AJ*, 80, 64
- . 1992, in *Mars*, ed. H. H. Kieffer et al. (Tucson: Univ. Arizona Press), 298
- Ward, W. R., Burns, J. A., & Toon, O. B. 1979, *J. Geophys. Res.*, 84, 243
- Ward, W. R., & de Campli, W. M. 1979, *ApJ*, 230, L117
- Ward, W. R., & Hamilton, D. P. 2004, *AJ*, 128, 2501 (WH)
- Yoder, C. F. 1995, in *Global Earth Physics*, ed T. J. Ahrens (Washington: Am. Geophys. Union), 1